

archives
of thermodynamics

Vol. 39(2018), No. 4, 125–140

DOI: 10.1515/aoter-2018-0033

Dynamic characteristics of the proton exchange membrane fuel cell module

JANUSZ T. CIEŚLIŃSKI^a,
TOMASZ Z. KACZMARCZYK^{b*}
BARTOSZ DAWIDOWICZ^a

^a Gdańsk University of Technology, Narutowicza 11/12, 80-233 Gdańsk, Poland

^b Institute of Fluid Flow Machinery, Polish Academy of Sciences, Fiszerka 14, 80-231 Gdańsk, Poland

Abstract The paper describes a fuel cell based system and its performance. The system is based on two fuel cell units, DC/DC converter, DC/AC inverter, microprocessor control unit, load unit, bottled hydrogen supply system and a set of measurement instruments. In the study presented in the paper a dynamic response of the proton exchange membrane (PEM) fuel cell system to unit step change load as well as to periodical load changing cycles in the form of semi-sinusoidal and trapezoidal signals was investigated. The load was provided with the aid of an in-house-developed electronic load unit, which was fully PC controlled. The apparatus was commissioned by testing the steady-state operation of the module. The obtained efficiency of the fuel cell shows that the test apparatus used in the study provides data in substantial agreement with the manufacturer's data.

Keywords: PEM fuel cell, hydrogen, dynamic characteristics

Nomenclature

ΔG – Gibbs free energy, kJ/kmol
 ΔH – Helmholtz free energy, kJ/kmol
 ΔS – entropy change, kJ/kmol K
 T – temperature, K

*Corresponding Author. Email: tkaczmarczyk@imp.gda.pl

Greek symbols η – efficiency**Subscripts** H – source L – sink th – thermodynamic

1 Introduction

Proton exchange membrane fuel cells (PEMFC) are viewed as one of the most environmentally friendly propulsion systems for automotive travel in the future. However, the output load and environmental conditions under which PEMFC operates are not constant. Thus, in order to provide references for the practical manufacture and operation of PEMFC, it is necessary to know the dynamic response of the PEMFC under variable loading and different operating conditions. Dynamic behavior of proton exchange membrane (PEM) fuel cell has not been investigated extensively. Due to the complex physics behind PEM fuel cell electrochemistry, the dynamic behaviors of PEM fuel cell have not been fully studied and understood.

Ottesen [1] studied dynamic behavior of Nexa power module using the resistor load-board. The resistor load-board was designed to provide a maximum load-current of about 40 A. Two high-current relays were used to independently switch the 1.3 Ω resistive units across the fuel cell output. Ottesen established that the Nexa power module can respond to load increases and load decreases of more than 40 A in less than 0.1 s or about 6 cycles at 60 Hz. Additionally the Nexa power module seemed to be emitting current ripples. Benziger *et al.* [2,3] revealed that dynamic response of a one-dimensional stirred tank reactor (STR PEM) fuel cell to changes in load exhibited steady-state multiplicity, resulting from a positive feedback between proton conduction in membrane and water production from the fuel cell reaction. The load resistance was varied from 0 to 25 Ω to obtain the polarization curve. Rodatz *et al.* [4] conducted tests with a hybrid fuel cell-powered vehicle during real-time operation. The vehicle (VW Bora) was equipped with supercapacitors for peak power levelling to assist the fuel cell during hard acceleration. The vehicle is powered by an alternating current (AC) motor with a permanent power output of 45 kW, peak power output of 75 kW, and a maximum torque of 225 Nm. Because of starvation phenomenon the current that is allowed to be imposed on the fuel cell needs

to be limited. The current was limited at 150 A and the dynamics of the fuel cell was limited to a conservative 2.5 kW/s. As further protection, the power demand on the fuel cell is reduced if any stack voltage drops below 70 V. Due to the constraints in the transient behavior of the fuel cell system, the fuel cell power is brought down with a gradient of 5 kW/s. Costa and Camacho [5] came to the conclusion that the coupling of a fuel cell with an inverter to produce alternating current is not a trivial task. The fuel cell as an energy source changes its internal parameters dynamically for each load or operating point. Additionally, the electrical resistor-capacitor (RC) time constant can change considerably with the control setup for the stack with all internal parameters inputs, and also shows that for a certain operating point, the RC constant during the load increase is larger than during the load decrease; opposite to the fact that the resistance in general increases with the value of current and temperature. Yan *et al.* [6] investigated both single fuel cell and stack configuration under variety of loading cycles and operating conditions. Different feed gas humidity, operating temperature, feed gas stoichiometry, air pressure, fuel cell size and gas flow patterns were found to affect the dynamic response of the fuel cell. The transient response measurement was performed by abruptly changing the current density and measuring the time response of the voltage across the fuel cell. The electronic load's minimum response time of 10 μs was sufficient for all dynamic tests performed on the fuel cell. It was found that the humidity of the cathode inlet gas had a significant effect on the fuel cell performance. The fuel cell steady-state and dynamic performance improved as the operating pressure was increased from 0.1 to 0.4 MPa. The experiment showed that an optimum air stoichiometry exists that is much larger than the stoichiometric value required for oxidation of the fuel. Thounthong *et al.* [7] tested 500 W PEM fuel cell connected with a power electronic converter. According to Thounthong *et al.* the results show the relative slowness of the fuel cell, which requires an auxiliary power source, such as battery or superconductor, in order to operate with high dynamics. Real *et al.* [8] investigated the start-up stage, constant load (to observe flooding effect), variable load (to analyze the transitory effects) and a long duration test with load changes of a 1.2 kW Ballard stack adjusting parameters. Real data from the tests were implemented in the developed model of the PEM fuel cell. Uzunoglu *et al.* [9] studied dynamic behavior and performance of a 5 kW fuel cell power plant equipped with a battery tank and a power conditioning unit. The following types of loads were used: resistive loads (resistive load bank),

inductive loads (transformers), resistive-inductive loads (washing machine), loads with high harmonic distortion (microwave and computers). Uzunoglu *et al.* concluded that the tested fuel cell power plant needs to be integrated with extra storage devices such as battery or ultra-capacitor bank to successfully meet all load demands. Yan *et al.* [10] conducted experiments with a 36 kW fuel cell test station (FCATAS-H36000) and a water-cooled electronic load system that had a maximum current of 1000 A. The loading response time of this electronic load was less than 0.1 s from 0 to 5000 A/m². The results show that the local current and temperature near the cathode inlet rise evidently when dynamic loading was applied. The temperature changes during dynamic loading were different at different air relative humidities. Chen and Zhou [11] tested a 10-cell commercial PEM fuel stack from Palcan Power System Inc. They established that when the air excess ratio was fixed at 2, the stack voltage experienced obvious and long-time oscillations after either the stack started from idle to a constant current load or stepped up from 1 A to an elevated current. Chen and Zhou proposed to utilize frequency of pressure drop signal as a diagnostic tool for PEM fuel stack dynamic behaviors. Corbo *et al.* [12,13] explored fuel cell system based on a 20 kW PEM stack integrated into the power train comprising DC-AC converter, Pb batteries as energy storage systems and asynchronous electric drive of 30 kW. The fuel cell system was able to support the dynamic requirements typical of European R40 cycle, but an increase of air flow rate during the fastest acceleration phases was necessary, with only a slight reduction of fuel cell system efficiency. The fuel cell system efficiency resulted was between 45% and 48%, while the overall power train efficiency reached 30% in conditions of constant stack power during the driving test. Tang *et al.* [14] employed commercial Nexa power module to investigate the dynamic behavior and transient response of a PEM fuel cell stack. Five groups of dynamic tests were conducted and divided into different stage such as start-up, shut-down, step-up load, regular load variation and irregular load variation. The transient responses of operating conditions, e.g., temperature, air flow rate, and current, reveal the complex interaction between related parameters and dynamic performance of PEM fuel cell, and disclose typical transient phenomena such as undershoot/overshoot effects, charge double-layer effect and purge effect. Wu *et al.* [15] discovered that the dynamic response performance of PEM fuel cell was improved by spraying RuO₂ × H₂O/CNTs composite material on the Pt/C catalyst of the cathode. When the fuel cell modi-

fied with $\text{RuO}_2 \times \text{H}_2\text{O}/\text{CNTs}$ was operated at lower pressure and higher air stoichiometry, a faster and more stable dynamic response could be found. It was also found that the humidity of cathode inlet gas had a significant effect on fuel cell performance. Adding 0.1 mg/cm^2 $\text{RuO}_2 \times \text{H}_2\text{O}/\text{CNTs}$ ($\text{RuO}_2 \times \text{H}_2\text{O}$ 11%) composite material not only slightly increases the single cell performance but also dramatically improves the dynamic response performance, revealing that $\text{RuO}_2 \times \text{H}_2\text{O}/\text{CNTs}$ can buffer the voltage undershoot whenever the current increases instantly. Hou *et al.* [16] tested a 45 kW fuel cell engine (FCE). An electronic load is used to provide load for FCE by controlling current, power, and voltage. The results show that the dynamic process of stack voltage responding to current step-up is different from that to current step-down. Additionally, the operating current values also have significant influence on the dynamic characteristics of stack voltage. Additionally, both the stack voltage overshoot and undershoot behaviors are observed when the stack current is step loaded, and the voltage variation rate decreases drastically in the first 20 s, and a higher operating current value will result in a higher voltage variation rate. Tang *et al.* [17] examined a 2 kW air-blowing fuel cell stack combined with a lead-acid battery pack during laboratory as well as road tests. The stack current and voltage respond transiently to the load variations when the fuel cell system itself is able to satisfy the power demand. When the external load is beyond the range of the fuel cell system, the battery begins to provide power assistance by increasing current output. The battery current exhibits satisfying transient responses to the load changes especially during the accelerating and climbing periods. Current overshoot and voltage undershoot are discovered during the transient process. The anodic operating pressure increases during the step-up and steady-state operations. Cho *et al.* [18] studied the transient response of a unit PEM fuel cell with a degraded gas diffusion layer (GDL). To age the GDL independently of the other components of PEM fuel cells and to reduce the aging time corresponding to the real operating time, an accelerated stress test, known as the leaching test was applied. Degradation of the GDL caused a 4.9% of performance decrease for a 100% of relative humidity (RH) condition and a 13.6% of performance decrease for a 50% of RH condition under standard stoichiometric conditions. The aged GDL showed a more unstable performance in low humidification conditions. The standard deviation of the voltage was about 0.03 V at a 50% of RH condition. The study suggests a correlation between the degradation effects of GDLs and the dynamic performance of

PEM fuel cells. By monitoring the amount of voltage response fluctuation at high current density, a diagnosis can be developed to detect the degradation of the GDL in situ. Outside automotive applications, PEM fuel cell may serve as stationary power supply system's [19].

Looking ahead, fuel cells with a power capacity up to 10 kW are expected to be used in small households [20]. However, the main barrier limiting the commercial use of fuel cells for energy purposes is their high price and the need to use highly energetic and high purity fuels (e.g. methane, hydrogen). Therefore, work is being carried out on the use of cheaper fuels (for example biofuels such as bioethanol and bio-oil) to supply solid oxide fuel cell (SOFC) and molten-carbonate fuel cell (MCFC) [21]. Research is also being carried out on the production processes of appropriate fuels and the use of stainless steel for the construction of components of direct carbon fuel cell (DCFCs) [22]. For instance, with an increase in air concentration from 21% to 30% in fuel at 3000 A/m², the efficiency of high temperature polymer electrolyte membrane fuel cells (HT-PEMFCs) increased by 8% [23]. However, one has to bear in mind that the operating temperature and appropriate load control in steady and transient states have a very significant impact on the efficiency and output power of a cell [24–26].

The primary aim of the study was to provide dynamic characteristics of the PEM fuel cell system that consisted of two Nexa power modules (1.2 kW each) connected in parallel, which complements the previous paper [27].

2 Polymer electrolyte fuel cell

Because of very high efficiency the PEM fuel cell is now the most promising technology for decentralized and small power systems. But the technology of manufacturing the polymer membranes is still under development. Polymer membrane fuel cells have the lowest working temperature, very seldom exceeding 373 K. To dissociate the hydrogen molecule at such low temperature there is a need to use a catalyst. Most widely used catalyst today is platinum (Pt) which is expensive and not resistant against carbon monoxide contamination. Because of this, fuel cell system working with PEM cells needs to be equipped with additional fuel cleaning devices, what rises the price of the whole system.

A fuel cell is an electrochemical cell which can continuously convert the chemical energy of a fuel and an oxidant to electrical energy by a process involving an essentially invariant electrode-electrolyte system, Fig. 1.

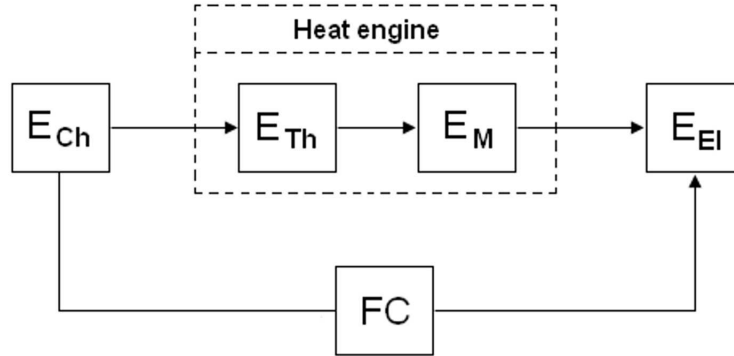


Figure 1: Direct energy conversion with fuel cell in comparison to conventional indirect technology: FC – fuel cell, E_{EI} – electrical energy (electricity), E_M – mechanical energy, E_{Ch} – chemical energy, E_{Th} – thermal energy.

Contradictory opinions have been formulated with regard to application of the second law of thermodynamics in fuel cell analysis of the theoretical performance potential. One group of researchers claims that the fuel cell is not a heat engine and therefore is not restricted by the second law of thermodynamics (Carnot limitation). Opponents argue that energy conversion during the fuel cell operation is restricted by the second law of thermodynamics because of heat exchange between fuel cell and the surroundings [28]. Exergy analysis conducted in [29] shows that fuel cell conversion is restricted by the second law of thermodynamics in the same way as heat engines.

An electrochemical energy converter (fuel cell), working ideally, has a thermodynamic efficiency given by [30]

$$\eta_{th} = \frac{\Delta G}{\Delta H} = 1 - \frac{T\Delta S}{\Delta H}, \quad (1)$$

where: ΔG – Gibbs free energy, ΔH – Helmholtz free energy, ΔS – entropy change.

It follows from Eq. (1) that if the entropy change of a reaction is negative (recalling the negative sign of ΔH) then the thermodynamic efficiency would decrease with an increase of temperature – Fig. 2. The performance of a heat engine operating between a source temperature, T_H , and a sink temperature, T_L , is limited by the Carnot efficiency

$$\eta_{th} = 1 - \frac{T_L}{T_H}. \quad (2)$$

It results from Eq. (2) that the thermodynamic efficiency of heat engine would increase with the increase of source temperature – Fig. 2. The con-

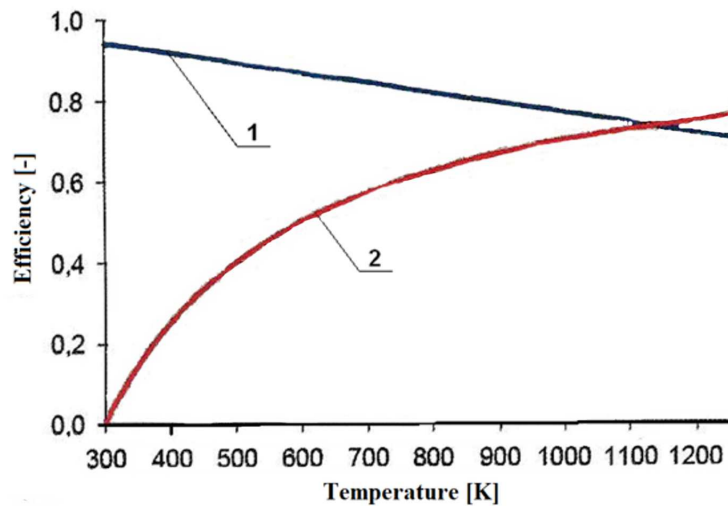


Figure 2: Comparison between the efficiency of Carnot cycle (2) and ideal fuel cell (1) [28].

trasting behaviour of thermal engines and fuel cethe temperature reduces some of the advantages of fuel cell at high temperatures. At higher temperature, however, the need for expensive electro catalysts is diminished because the temperature itself increases the reaction rate, and therefore makes the overpotential necessary for providing a given current density less than that at lower temperature [31].

3 Fuel cell module

The scheme of the tested PEM fuel cell system is shown in Fig. 3. All experiments were conducted in the Laboratory of Ecoenergy of the Gdańsk University of Technology. The module tested is based on two fuel cell units 1.2 kW each produced by Ballard Power Systems Inc. and called Nexa. The Nexa power module produces unregulated DC power for interfacing with external power conditioning equipment. A single fuel cell element produces about 1 V at an open-circuit and about 0.6 V at full current output. The Nexa fuel cell stack has a total of 47 fuel cells in series. The geometric area of the single cell is equal to 120 cm² [32]. To determine the

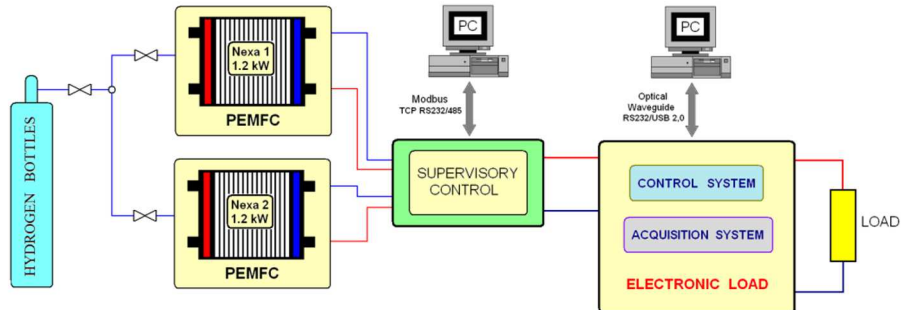


Figure 3: Schematic diagram of the 2×1.2 kW PEM fuel cell system.

dynamic characteristics of the tested PEM fuel cell system an electronic load system was designed and constructed. The system is composed of board of interfaces AMT 022, control board of the type SH65L with a microprocessor ADSL21065L. Actuator adjustment module consists of four transistors of a type PM50RLA120 on a bridge. The controlled variable is the output current from the fuel cell. Current measurement is carried out through the current transducers LEM of the type LA 55P/ SP1. The load system consists of the elements of a resistive-inductive (RL) types – Fig. 4. To visualize the results as well as a console to control the test system a PC computer is used. Control of the load is carried out using a specially designed control panel. The applied program allows to control the load current of a given period and waveform (triangular, rectangular, sinusoidal, trapezoidal and unit step).

4 Results and discussion

4.1 Steady state characteristics

Ignition/extinction is indicative of multiple steady states in PEM fuel cell operation (the same reactor conditions, feed flow rates, temperature and load resistance can result in two different stable operating states). The steady state polarization curve displayed in Fig. 5 shows regions where there are either stable steady states that could exist for the same set of operating parameters (feed flow rate, temperature and load resistance). Present results are in good agreement with manufacturer's [32] and Yilanci data [33]. Figure 6 shows comparison of the efficiencies of the module Nexa

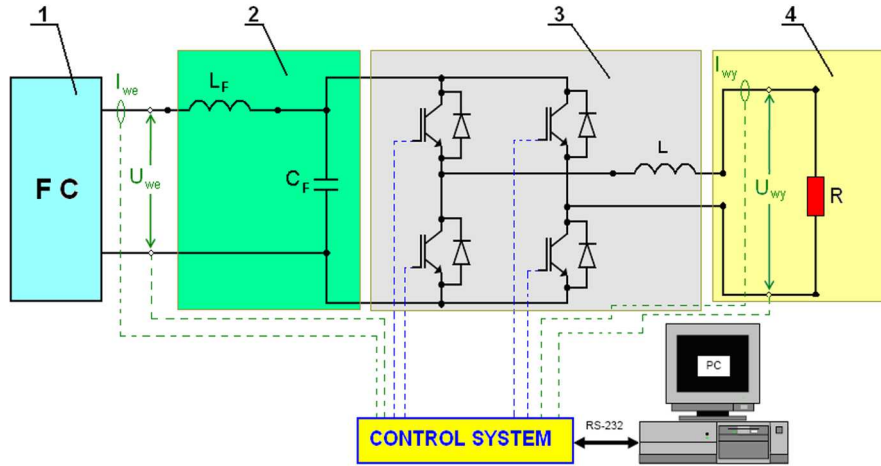


Figure 4: Scheme of the PEMFC system: 1 – FC module, 2 – filter, 3 – electronic load system, 4 – resistive load.

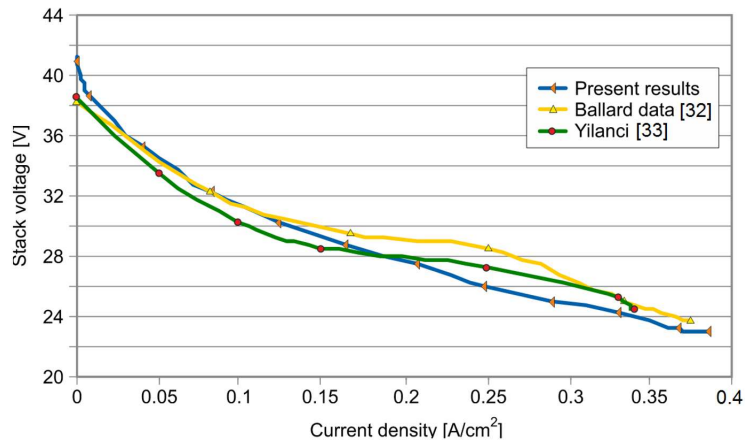


Figure 5: Steady-state characteristics.

gathered during the research and the efficiency according to the manufacturer's data, company Ballard. Maximum fuel stack efficiency obtained – for minimum load, was almost 60%. Because of internal loads module efficiency was about 13% lower than the stack efficiency. Both stack efficiency and module efficiency decrease with the load increase.

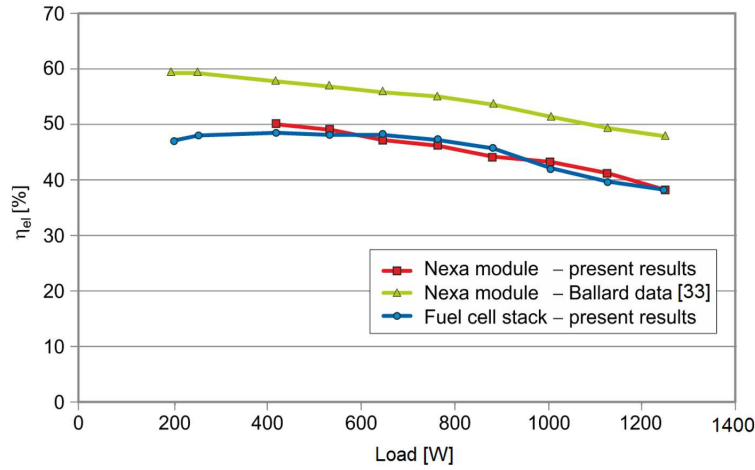


Figure 6: Efficiency of the module Nexa1 versus power output.

4.2 Dynamic characteristics

As an example Fig. 7 shows current response under unit step change – from idle to 15 A load of two Nexa power modules connected parallel. Green and red lines illustrate input and output signal, respectively.

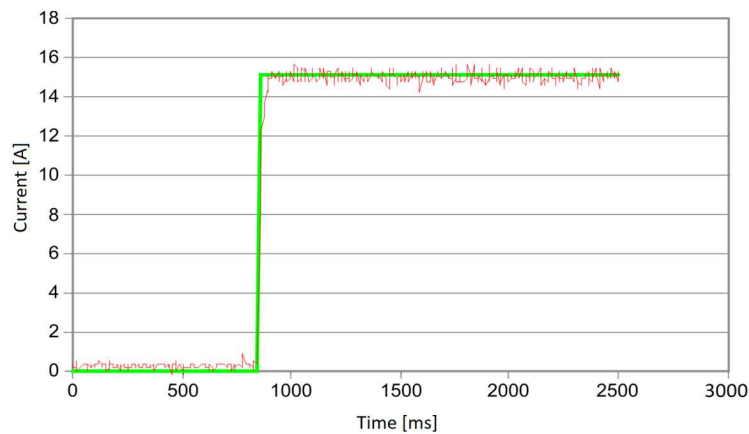


Figure 7: Current response of the system of two Nexa power modules connected parallel under the unit step change (15 A).

Figure 8 displays corresponding current difference between input and output signals versus time. Figure 7 shows after very short time that the

investigated Nexa system follows the load signal very faithfully and maximum current difference between input and output signal is equal to 7.5 A – Fig. 8.

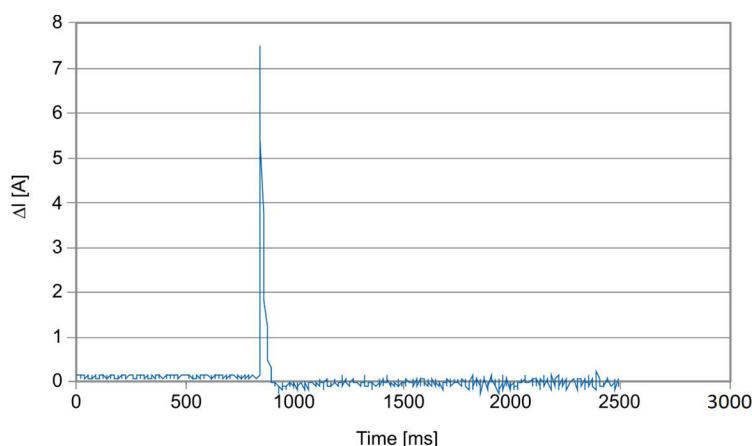


Figure 8: Current difference between the load and response signal of two Nexa power modules connected parallel under the unit step change (15 A).

Figure 9 illustrates current response of the two Nexa power modules when a semi-sinusoidal load signal with amplitude 15 A and period 1000 ms is applied. Figure 10 shows the current difference between load and response signal. Figure 11 illustrates current response of the two Nexa modules when trapezoidal load signal with amplitude 25 A, period 15000 ms and ramp 1400 ms is applied. As in the case of the unit step change signal, the Nexa module follows load signal faithfully.

5 Summary and conclusions

1. The apparatus was commissioned by testing the single Nexa power module steady-state. Obtained efficiency of the fuel cell shows that test apparatus used in present study provides data in substantial agreement with the manufacturer's data.
2. The modules tested have quite big internal loads. For the nominal power of 1.2 kW almost 300 W needs to be used to keep the system working. This fact dramatically reduces the overall efficiency that could be as high as 59% for zero internal loads.

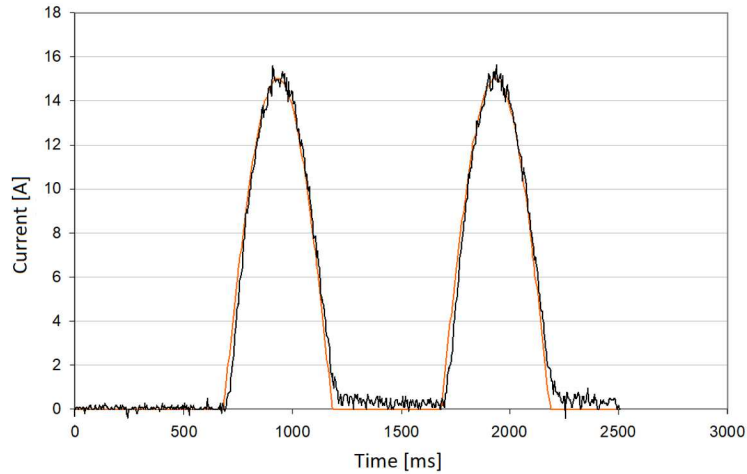


Figure 9: Current response of the two Nexa power modules for semi-sinusoidal load signal with amplitude 15 A and period 1000 ms.

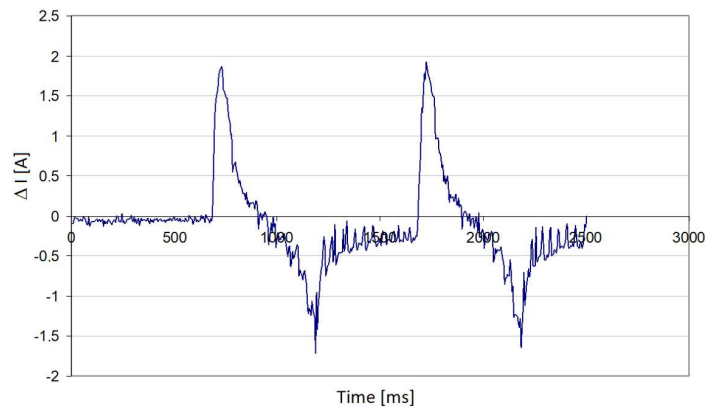


Figure 10: Current difference between load and response signal of two Nexa modules connected in parallel for semi-sinusoidal load signal with amplitude 15 A and period 1000 ms.

3. Electrical current generated in the fuel cell module is in linear correlation with the hydrogen consumption.
4. System examined displays sustained operation within broad range of current load from 1 A to 50 A.
5. Time needed to reach a steady-state performance from idle to 1 A,

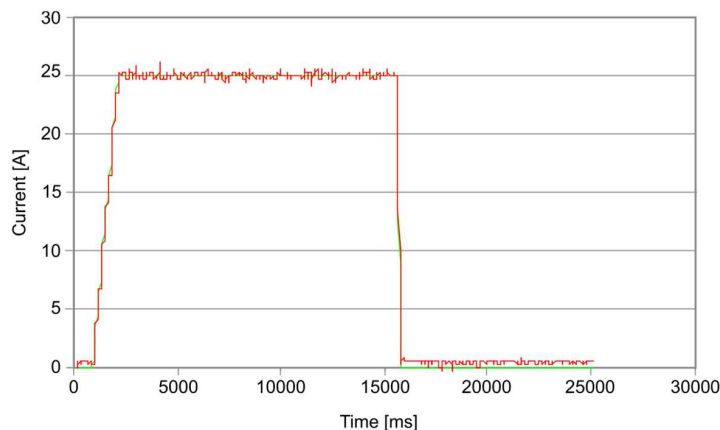


Figure 11: Current response of the two Nexa modules for trapezoidal load signal with an amplitude 25 A, period 15000 ms and ramp 1400 ms.

5 A, 30 A, 45 A, and 50 A load was very short – from 60 ms to 430 ms for 30 A and 50 A, respectively.

6. Listed above features make the proton exchange membrane fuel cell as promising and attractive candidate for electric vehicle power.

Received 20 April 2018

References

- [1] OTTESEN H.H.: *Dynamic Performance of the Nexa Fuel Cell Power Module*. Uni. Minnesota, 2004.
- [2] BENZIGER J., CHIA E., MOXLEY J.F., KEVREKIDIS I.G.: *The dynamic response of PEM fuel cells to change in load*. Chem. Eng. Sc. **60**(2005), 1743–1759.
- [3] BENZIGER J.B. ET AL.: *The stirred tank reactor polymer electrolyte membrane fuel cell*. AIChE J. **50**(2004), 1889–1899.
- [4] RODATZ P., PAGANELLI G., SCIARETTA A., GUZELLA L.: *Optimal power management of an experimental fuel cell/supercapacitor-powered hybrid vehicle*. Control Eng. Pract. **13**(2005), 41–53.
- [5] COSTA R.A., CAMACHO J.R.: *The dynamic and steady-state behaviour of a PEM fuel cell as an electric energy source*. J. Power Sources **161**(2006), 1176–1182.
- [6] YAN Q., TOGHIANI H., CAUSEY H.: *Steady state and dynamic performance of proton exchange membrane fuel cell (PEMFCs) under various operating conditions and load changes*. J. Power Sources **161**(2006), 492–502.

- [7] THOUNTHONG P., RAËL S., DAVAT B.: *Test of a PEM fuel cell with low voltage static converter*. J. Power Sources **153**(2006), 145–150.
- [8] REAL A.J., ARCE A., BORDONS C.: *Development and experimental validation of a PEM fuel cell dynamic model*. J. Power Sources **173**(2007), 310–324.
- [9] UZUNOGLU M., ONAR O.C., ALAM M.S.: *Dynamic behaviour of PEM FCPPs under various load conditions and voltage stability analysis for stand-alone residential applications*. J. Power Sources **168**(2007), 240–250.
- [10] YAN Y. ET AL.: *The study on transient characteristic of proton exchange membrane fuel cell stack during dynamic loading*. J. Power Sources **163**(2007), 966–970.
- [11] CHEN J., ZHOU B.: *Diagnosis of PEM fuel cell stack dynamic behaviour*. J. Power Sources **177**(2008), 83–95.
- [12] CORBO P., MIGLIARDINI F., VENERI O.: *An experimental study of a PEM cell power train for urban bus application*. J. Power Sources **181**(2008), 363–370.
- [13] CORBO P., MIGLIARDINI F., VENERI O.: *Experimental analysis of a 20 kW PEM fuel cell system in dynamic conditions representative of automotive applications*. Energ. Convers. Manage. **49**(2008), 2688–2697.
- [14] TANG Y., YUAN W., PAN M., LI Z., CHEN G., YONG LI Y.: *Experimental investigation of dynamic performance and transient responses of a kW-class PEM fuel cell stack under various load changes*. Appl. Energ. **87**(2010), 1410–1417.
- [15] WU X., XU H., LU L., FU J., ZHAO H.: *The study on dynamic response performance of PEMFC with RuO₂-xH₂O/CNTs and Pt/C composite electrode*. Int. J. Hydrogen Energ. **35**(2010), 2127–2133.
- [16] HOU Y., YANG Z., XUE FANG X.: *An experimental study on the dynamic process of PEM fuel cell stack voltage*. Renew. Energ. **36**(2011) 325–329.
- [17] TANG Y., YUAN W., PAN M., WAN Z.: *Experimental investigation on the dynamic performance of a hybrid PEM fuel cell/battery system for lightweight electric vehicle application*. Appl. Energ. **88**(2011), 68–76.
- [18] CHO J. ET AL.: *Analysis of transient response of a unit proton-exchange membrane fuel cell with a degraded gas diffusion layer*. Int. J. Hydrogen Energ. **36**(2011), 6090–6098.
- [19] BUJLO P., PASCIAK G., CHMIELOWIEC J., MALINOWSKI M.: *Application of a polymer exchange membrane fuel cell stack as the primary energy source in a commercial uninterruptible power supply unit*. J. Power Technol. **93**(2013), 3, 154–160.
- [20] MILEWSKI J., BUDZIANOWSKI W.: *Recent key technical barriers in solid oxide fuel cell technology*. Arch. Thermodyn. **35**(2014), 1, 17–41, DOI: 10.2478/aoter-2014-0002.
- [21] MILEWSKI J., BUJALSKI W., LEWANDOWSKI J.: *Thermodynamic analysis of biofuels as fuels for high temperature fuel cells*. Arch. Thermodyn. **33**(2012), 4, 41–65, DOI: 10.2478/v10173-012-0027-7
- [22] KACPRZAK A., KOBYLECKI R., BIS Z.: *Clean energy from a carbon fuel cell*. Arch. Thermodyn. **32**(2011), 3, 145–155, DOI: 10.2478/v10173-011-0019-z

- [23] PINAR F. J., RASTEDT M., DYCK A., WAGNER P.: *Long-term operation of high temperature polymer electrolyte membrane fuel cells with fuel composition switching and oxygen enrichment*. Fuel Cell **18**(2018), 3, <https://doi.org/10.1002/fuce.201700115>
- [24] SZMYD J.S., KOMATSU Y., BRUS G., GHIGLIAZZA F., KIMIJIMA S., ŚCIAŻKO A.: *The effect of applied control strategy on the current-voltage correlation of a solid oxide fuel cell stack during dynamic operations*. Arch. Thermodyn. **35**(2014), 3, 129–143, DOI: 10.2478/aoter-2014-0025.
- [25] KACPRZAK A., KOBYLECKI R., BIS Z.: *The effects of operating conditions on the performance of a direct carbon fuel cell*. Arch. Thermodyn. **34**(2013), 4, 187–197, DOI: 10.2478/aoter-2013-0037
- [26] BVUMBE T.J., BUJLO P, TOLJ I., MOUTON K., SWART G., PASUPATHI S., POLLET B.G.: *Review on management, mechanisms and modelling of thermal processes in PEMFC*. Hydrogen and Fuel Cells, **1**(2016), 1–20.
- [27] CIEŚLIŃSKI J.T, KACZMARCZYK T.Z., DAWIDOWICZ B.: *Performance of the PEM fuel cell module. Part 2. Effect of excess ratio and stack temperature*. J. Power Technol. **97**(2017), 3, 246–251.
- [28] PIÓRO D.: *Introduction to thermodynamic analysis of fuel cells*. TChiK **1–2**(2010), 5–9 (in Polish).
- [29] WRIGHT S.E.: *Comparison of the theoretical performance potential of fuel cells and heat engines*. Renew. Energ. **29** (2004), 175–195.
- [30] HOLMAN J.P.: *Thermodynamics*. McGraw-Hill New York, 1980.
- [31] KORDESCH K., SIMADER G.: *Fuel Cells and their Applications*. VCH, Weinheim, 1996.
- [32] *Nexa Power Module User's Manual*. Ballard Power Systems, June 2003.
- [33] YILANCI A., OZTURK H.K., ATALAY O., DINCER I.: *Exergy analysis of a 1.2 kW PEM fuel Cell system*. In: Proc. 3rd Int. Energy, Exergy and Environmental Symp., Evora 2007.